Numerical Study of Heat Transport in Static Liquid Metal Exposed to Plasma with Magnetic Field*)

Nopparit SOMBOONKITTICHAI†) and Guizhong ZUO[1)]

Department of Physics, Faculty of Science, Kasetsart University, Chatuchak, Bangkok 10900, Thailand
[1)]*Institute of Plasma Physics, Chinese Academy of Sciences, Hefei 230031, China*

(Received 9 January 2023 / Accepted 6 March 2023)

Suitable management of excessive heat in liquid metal is one of key roles to accomplish the proper liquid metal usage as future alternative fusion plasma facing components. In this work, theoretical heat transfer in liquid metal in contact with magnetized plasma was carried out, and a numerical solver for investigating temperature and induced velocity by $\mathbf{j}\times\mathbf{B}$ force has been developed. The study suggests the trends: 1. lower bulk temperature in liquid metal at which magnetic field is presented, compared to no magnetic field, by additional convection from $\mathbf{j}\times\mathbf{B}$, stronger than natural convection; and 2. asymmetric temperature distribution in liquid metal along $\mathbf{j}\times\mathbf{B}$.

Keywords: plasma surface interactions, plasma facing components, magnetized plasma, liquid metal, magneto-hydrodynamics, Maxwell's equation, natural convection, heat conduction, generalized Ohm's law

DOI: 10.1585/pfr.18.2403027

1. Introduction

Plasma facing components (PFCs) made of liquid metals (LM), which are low in melting point but compatible with fuel, are considered to be a candidate for being inner surfaces of next step fusion device in long-run operations [1]. Several experiments have investigated the use of lithium (Li) [2–12], tin (Sn) [13, 14], gallium (Ga) [15, 16] and LiSn (lithium-tin alloy) [17, 18] as PFCs. The experiments investigated the bombardment of plasma on LM samples suggested the depletion of LM amount [10], which releases as LM vapor. In addition, the LiMIT system, one of currently implemented feeding structures of LM, is relied on temperature gradient in LM to produce an extra force to drive LM flowing in guiding grooves [19,20]. About experimental thermal analysis, thermocouple system with numerical analysis, via ANSYS, investigating gas cooling in FLiLi has been reported in [21].

Understanding heat transfer in LM exposed to magnetized plasma helps in advancing the methodology of guiding LM as PFCs and controlling their working temperatures in a power-plant fusion device. The current study has been focused on theoretically investigating heat transfer in LM in magnetized plasma. The numerical solver was implemented to study a static rectangular liquid conductor exposed to a magnetized plasma. The physical models exploited are outlined in section 2. The assumption used in developing the numerical solver are mentioned in section 3. The preliminary result is presented and discussed in section 4. The last section concludes the current study.

author's e-mail: †)*fscinrso@ku.ac.th,* [1)]*zuoguizh@ipp.ac.cn*

*) This article is based on the presentation at the 31st International Toki Conference on Plasma and Fusion Research (ITC31).

2. Physical Model

The exploited physical models are the momentum equation [22] with Boussineq's approximation [23] for a buoyant force to be taken into account, generalized Ohm's law [24] and convective heat equation [25], respectively, as follows

$$\rho\left(\frac{\partial \mathbf{v}}{\partial t}+(\mathbf{v}\cdot\nabla)\mathbf{v}\right)=\mathbf{j}\times\mathbf{B}-\mathbf{g}\rho\beta(T-T_{ref}), \tag{1}$$

$$\mathbf{E}+\mathbf{v}\times\mathbf{B}=\eta\mathbf{j}, \tag{2}$$

$$\frac{\partial T}{\partial t}+(\mathbf{v}\cdot\nabla)T=\frac{k}{\rho c}\nabla^2 T+\frac{Q}{\rho c}, \tag{3}$$

where $\mathbf{j}$ is current density, $\mathbf{v}$ is liquid velocity, $\mathbf{g}$ is gravitational acceleration, $\mathbf{B}$ is external magnetic field, $\mathbf{E}$ is electric field, ρ is liquid density, β is volumetric thermal expansion coefficient at reference temperature (T_{ref}), T is liquid temperature, η is electrical resistivity, k is thermal conductivity, c is specific heat capacity, and Q is source/sink power density.

Using $\mathbf{E}=-\nabla\phi$ [24], where ϕ is electrical potential, and equation 2, equation 1 becomes

$$\frac{\partial \mathbf{v}}{\partial t}+(\mathbf{v}\cdot\nabla)\mathbf{v}=\frac{1}{\rho\eta}\left[(-\nabla\phi\times\mathbf{B})+(\mathbf{v}\times\mathbf{B})\times\mathbf{B}\right]-\mathbf{g}\beta(T-T_{ref}). \tag{4}$$

Using charge continuity, i.e. $\nabla\cdot\mathbf{j}=0$ [24], in equation 2,

$$\nabla^2\phi=\nabla\cdot(\mathbf{v}\times\mathbf{B}). \tag{5}$$

3. Numerical Modeling

Equations 3 - 5 are mainly solved by discretization using Leapfrog scheme [26] for T, $\mathbf{v}$ and ϕ, respectively.

Liquid is assumed to be isotropic, so that approximately $\beta = 3\alpha$, where α is linear thermal expansion coefficient. Bulk heat source is Joule heating power density, i.e. $Q = \eta j^2$ [24], where j is the magnitude of current density.

Plasma deposits both energy and charges on liquid boundary. This sets up electrical potential (ϕ) and particle heat flux (Ξ) at the liquid surface. The expressions of ϕ and Ξ [27] are

$$\phi \approx -2T_e[\text{eV}], \tag{6}$$

$$\Xi \approx 6.83neT_e[\text{eV}]v_s, \tag{7}$$

where T_e[eV] is electron temperature, n is number density of quasi-neutral plasma, e is elementary charge, and v_s is ion sound speed. Thermal radiation and evaporation are adopted as cooling. The current version of the numerical solver has yet to account for coolant flow, and vapor release and their associated formation of shielding. Therefore, the temperature of the liquid becomes larger than usual.

A liquid is assumed to be in a rectangular shape, where the X, Y and Z-axes represent the coordinates in the directions of width, length and thickness, with fixed boundaries, in thermal equilibrium with the liquid. This results in that the X- and Y-directions represent the horizontal directions of the liquid, but the Z-direction represents the upward vertical direction of the liquid, parallel to the surface normal. The initial temperature of the liquid is its melting temperature. A plasma is in contact with only the top XY-plane boundary and both YZ-plane boundaries. Except the top XY-plane boundary of the liquid, no-skip condition is applied at the rest boundaries, i.e. $\mathbf{v} = 0$. In figures 1 and 2, it must be noted that the reason why the magnitudes of velocities very close to the boundaries of the middle XZ-, YZ- and XY-planes illustrate non-zero magnitude is because the current version of the code put the no-skip condition in the ghost grid-points at the boundaries and has yet to include the flow boundary layer adjacent to the boundaries. Inviscid liquid is currently considered.

4. Results and Discussion

Liquid lithium (Li) is considered as liquid metal (LM) in the current study. The size are 5 cm in width and length, and 2 mm in thickness. LM is presumably static at the beginning. Plasma is deuterium (D) with $n = 10^{18}$ m^{-3} and $T_e = 10$ eV. External magnetic field strength are zero and 1 T with the inclination of 87° to the normal direction of the liquid top surface, i.e. $\mathbf{B} = (0.9986, 0, -0.0014)$ T. The direction of $\mathbf{B}$ with such an angle corresponds to the open magnetic field next to limiter and divertor targets in tokamaks [27].

As shown in Fig. 1, without magnetic field, buoyant force induces small velocity mainly in the Z-direction, i.e. natural convection. The liquid velocity is in the upward direction in parallel to the gravitational acceleration. In contrast, with magnetic field, the bulk horizontal velocity is greatly induced to reach a few hundreds m/s. Such velocity originates from $\mathbf{j} \times \mathbf{B}$ force, and it is in the direction perpendicular to $\mathbf{j}$ and $\mathbf{B}$, as seen in Fig. 2. In case of no $\mathbf{B}$, current density (j), contributed from conduction, is due to the transport of deposited charges, contributed

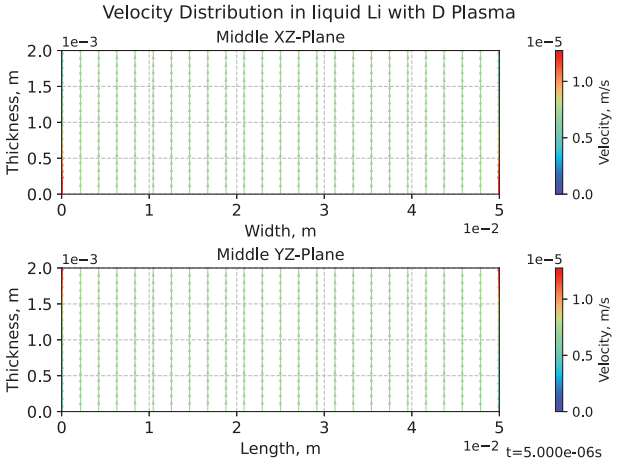

Fig. 1 Velocity distribution in liquid Li exposed to unmagnetized plasma, considered at middle cross-section of liquid Li slab.

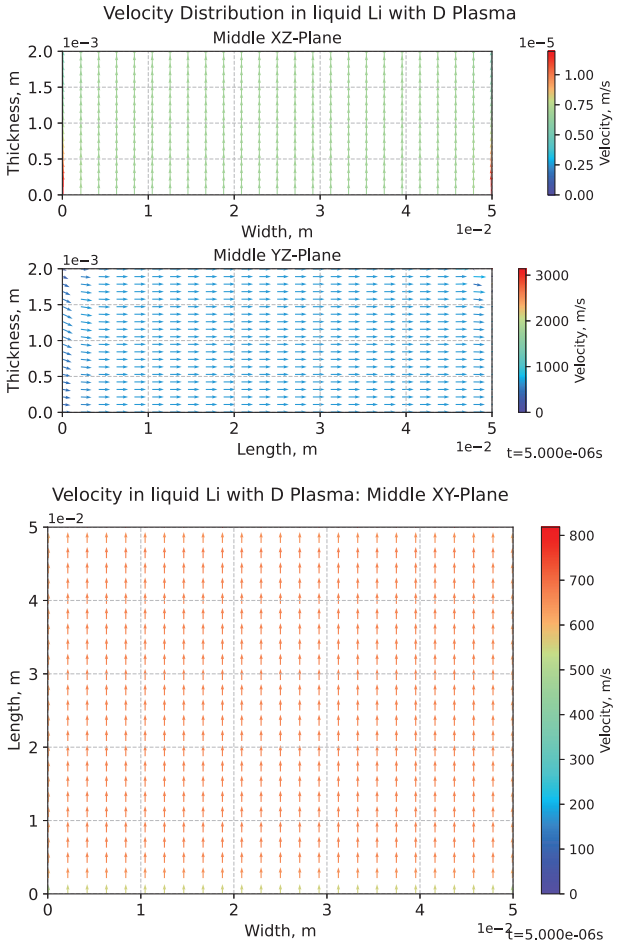

Fig. 2 Velocity distribution in liquid Li exposed to magnetized plasma of 1 T, with 87° inclination to surface normal, considered at middle cross-section of liquid Li slab.

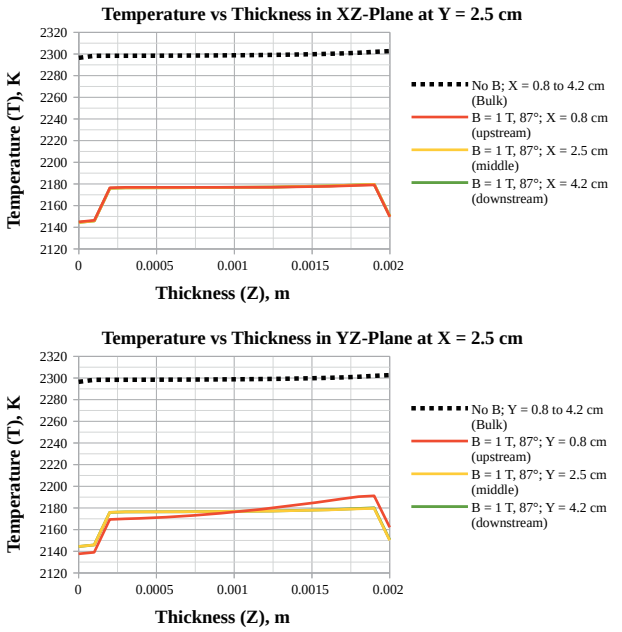

Fig. 3 Temperature distribution in liquid Li, exposed to magnetized (B = 1 T, 87° inclination to surface normal) and unmagnetized plasmas at XZ- and YZ-planes at middle of slab in X- and Y-directions corresponding to velocity distribution shown in Figs. 1 and 2.

from plasma bombardment, from the liquid top (XY-plane) and side (YZ-plane) surfaces, electrically floating by ϕ, to zero-grounded potential underneath the liquid, i.e. under the effect of inner electric field. Its direction is mainly in the vertical direction. Near the YZ-plane boundaries, it is bent in a short distance before it is directed vertically by inner electric field. For non-zero **B**, current density, provided by convection, is added to the conduction one. This causes stronger j in the vertical direction of bulk LM, and then this leads to the larger in-liquid power source.

Due to the extra motion provided by $\mathbf{j} \times \mathbf{B}$, temperature gradient tends to be leveled off inside LM. Near the plasma contacting surface, LM is relatively high in temperature due to plasma bombardment. In Fig. 3, under the coordinate system of the current study, the direction of $\mathbf{j}\times\mathbf{B}$ is in the Y-direction, as illustrated in Fig. 2. The presence of $\mathbf{j}\times\mathbf{B}$ allows temperature across the liquid thickness to be lower than that of no magnetic field for the bulk XZ-plane region, i.e. $0.8 \leq X \leq 4.2$ cm approximately, and the bulk YZ-plane region, i.e. $0.8 \leq Y \leq 4.2$ cm approximately. In the bulk XZ-plane region, all temperatures are near the same at the same depth in its thickness. This suggests uniform temperature distribution. In contrast, in the bulk YZ-plane region, i.e. $0.8 \leq Y \leq 4.2$ cm approximately, the upstream region, e.g. $Y = 0.8$ cm, is larger in near-surface temperature than those of the middle, i.e. $Y = 2.5$ cm, and the downstream, e.g. $Y = 4.2$ cm, regions. The gradient of inner temperature of the upstream region is steeper than those of the middle and the downstream regions. This suggests the asymmetric temperature distribution, achieved by horizontal induced flow provided by $\mathbf{j} \times \mathbf{B}$. The induced flow contributed from $\mathbf{j} \times \mathbf{B}$ tends to transport heat, associated with plasma bombardment, in the upstream region, and leads to mixing along the way to the downstream region. This levels off the trends of the near-surface temperature in the downstream region.

Beneficial to the design of LM coolant management, the current study may suggest that the coolant flow, e.g. underneath the liquid Li slab, should be made in parallel flow along the $\mathbf{j} \times \mathbf{B}$ direction in order to cool down the upstream LM as priority.

5. Conclusion

The heat transfer numerical solver, consisting of momentum equation, generalized Ohm's law and convective heat equation, has been developed to predict the trends of the temperature distribution and the induced liquid velocity under the presence of magnetized plasma. Apart from plasma bombardment as an external heat source, an internal heat source by Joule heating inside the liquid conductor was included. The plasma parameters, as boundary conditions, considered in the study are of typical edge fusion plasmas.

Even though, a non-moving liquid metal (LM) is initially implemented in a magnetized plasma, a horizontal flowing is then induced by $\mathbf{j} \times \mathbf{B}$, additional to vertically upward natural convection by buoyancy. This means that static LM is hardly to be achieved in a magnetized plasma, and unavoidably, its heat transfer is not in the conduction but the convection regimes. The study suggests that the induced horizontal velocity by $\mathbf{j} \times \mathbf{B}$ is relatively large.

The inner temperature of LM becomes lower in the presence of $\mathbf{j}\times\mathbf{B}$ than the case of no magnetic field. Moreover, the upstream region at which the direction is in parallel to $\mathbf{j} \times \mathbf{B}$ is larger in near-surface temperature compared to the middle and the downstream regions. Therefore, the temperature asymmetrically distributes in LM caused by convective mixing. Consequently, this suggests the requirement that the coolant flow should be in the same direction as $\mathbf{j}\times\mathbf{B}$. This is in order to cool the upstream down.

It has to be noted that the current heat transfer solver has not included sophisticated models of coolant pumping, and vapor release and its shielding effect. Therefore, only the magnitudes of temperature and induced flow velocity may be overestimated but should not be for their trends.

Acknowledgements

N. Somboonkittichai attended the 31st International Toki Conference on Plasma and Fusion Research (ITC31) and produced this work, as the contribution to ITC31, supported by Grant No. RGNS 63-047, provided by the Office of the Permanent Secretary, Ministry of Higher Education, Science, Research and Innovation (OPS MHESI), Thailand, Thailand Science Research and Innovation (TSRI), and Kasetsart University (KU, Bangkok, Thailand). G.

Z. Zuo was supported by the National Key Research and Development Program of China (2017YFE0301100, 2022YFE03130000) and Interdisciplinary and Collaborative Teams of CAS. N. Somboonkittichai deeply appreciates J. Nakamura (JAEA, Japan) for good discussions on liquid metal, and S. Aiemkong and S. Somboonkittichai for encouragement. T. Onjun, Executive Director of Thailand Institute of Nuclear Technology (TINT), provided general supervision to N. Somboonkittichai.

[1] R. Nygren and F. Tabarés, "Liquid surfaces for fusion plasma facing components—a critical review. part i: Physics and psi", Nucl. Mater. Energy **9**, 6 (2016).

[2] J. Hu, G. Zuo, J. Li, N. Luo, L. Zakharov, L. Zhang, W. Zhang and P. Xu, "Investigation of lithium as plasma facing materials on ht-7", Fusion Eng. Des. **85**, no. 6, 930 (2010).

[3] G. Zuo, J. Hu, J. Li, N. Luo, L. Zakharov, L. Zhang and A. Ti, "First results of lithium experiments on east and ht-7", J. Nucl. Mater. **415**, no. 1, Supplement, S1062 (2011).

[4] J. Hu, J. Ren, Z. Sun, G. Zuo, Q. Yang, J. Li, D. Mansfield, L. Zakharov and D. Ruzic, "An overview of lithium experiments on ht-7 and east during 2012", Fusion Eng. Des. **89**, no. 12, 2875 (2014).

[5] G. Zuo, J. Ren, J. Hu, Z. Sun, Q. Yang, J. Li, L. Zakharov and D.N. Ruzic, "Liquid lithium surface control and its effect on plasma performance in the ht-7 tokamak", Fusion Eng. Des. **89**, no. 12, 2845 (2014).

[6] J. Ren, J.S. Hu, G.Z. Zuo, Z. Sun, J.G. Li, D.N. Ruzic and L.E. Zakharov, "First results of flowing liquid lithium limiter in HT-7", Physica Scripta **T159**, 014033 (2014).

[7] G. Zuo, C. Li, R. Maingi, X. Meng, D. Andruczyk, P. Sun, Z. Sun, W. Xu, M. Huang, Z. Tang, D. Zhang, Y. Chen, Q. Zang, Y. Wang, Y. Wang, K. Tritz and J. Hu, "Effect of continuously flowing liquid li limiter on particle and heat fluxes during h-mode discharges in east", Nucl. Mater. Energy **33**, 101263 (2022).

[8] A. Vertkov, I. Lyublinski, F. Tabares and E. Ascasibar, "Status and prospect of the development of liquid lithium limiters for stellarotor tj-ii", Fusion Eng. Des. **87**, no. 10, 1755 (2012).

[9] F.L. Tabarés, E. Oyarzabal, D. Tafalla, A. Martin-Rojo, D. Alegre and A. de Castro, "First liquid lithium limiter biasing experiments in the tj-ii stellarator", J. Nucl. Mater. **463**, 1142 (2015).

[10] S. Mirnov and V. Evtikhin, "The tests of liquid metals (ga, li) as plasma facing components in t-3m and t-11m tokamaks", Fusion Eng. Des. **81**, no. 1, 113 (2006).

[11] I.E. Lyublinski and A.V. Vertkov, "Experience and technical issues of liquid lithium application as plasma facing material in tokamaks", Fusion Eng. Des. **85**, no. 6, 924 (2010).

[12] S. Mirnov, E. Azizov, A. Alekseev, V. Lazarev, R. Khayrutdinov, I. Lyublinski, A. Vertkov and V. Vershkov, "Li experiments on t-11m and t-10 in support of a steady-state tokamak concept with li closed loop circulation", Nucl. Fusion **51**, 073044 (2011).

[13] G. Mazzitelli, M. Apicella, M. Iafrati, G. Apruzzese, F. Bombarda, F. Crescenzi, L. Gabellieri, A. Mancini, M. Marinucci and A. Romano, "Experiments on the Frascati tokamak upgrade with a liquid tin limiter", Nucl. Fusion **59**, 096004 (2019).

[14] A. Vertkov, I. Lyublinski, M. Zharkov, G. Mazzitelli, M. Apicella and M. Iafrati, "Liquid tin limiter for ftu tokamak", Fusion Eng. Des. **117**, 130 (2017).

[15] R. Gomes, H. Fernandes, C. Silva, A. Sarakovskis, T. Pereira, J. Figueiredo, B. Carvalho, A. Soares, C. Varandas, O. Lielausis, A. Klyukin, E. Platacis and I. Tale, "Interaction of a liquid gallium jet with the tokamak isttok edge plasma", Fusion Eng. Des. **83**, no. 1, 102 (2008).

[16] R. Gomes, H. Fernandes, C. Silva, A. Sarakovskis, T. Pereira, J. Figueiredo, B. Carvalho, A. Soares, P. Duarte, C. Varandas, O. Lielausis, A. Klyukin, E. Platacis, I. Tale, and A. Alekseyv, "Liquid gallium jet–plasma interaction studies in isttok tokamak", J. Nucl. Mater. **390-391**, 938 (2009).

[17] V.P. Krasin and S.I. Soyustova, "Important thermodynamic parameters of lithium-tin alloys from the point of view of their use in tokamaks", High Temperature **57**, no. 2, 190 (2019).

[18] I. Tazhibayeva, Y. Ponkratov, I. Lyublinsky, Y. Gordienko, A. Vertkov, Y. Tulubayev, K. Samarkhanov, V. Bochkov, Y. Kozhakhmetov and N. Orazgaliyev, "Study of liquid tin-lithium alloy interaction with structural materials of fusion reactor at high temperatures", Nucl. Mater. Energy **30**, 101152 (2022).

[19] D. Ruzic, W. Xu, D. Andruczyk and M. Jaworski, "Lithium–metal infused trenches (limit) for heat removal in fusion devices", Nucl. Fusion **51**, 102002 (2011).

[20] D. Ruzic, M. Szott, C. Sandoval, M. Christenson, P. Fiflis, S. Hammouti, K. Kalathiparambil, I. Shchelkanov, D. Andruczyk, R. Stubbers, C. J. Foster and B. Jurczyk, "Flowing liquid lithium plasma-facing components – physics, technology and system analysis of the limit system", Nucl. Mater. Energy **12**, 1324 (2017).

[21] X. Meng, M. Huang, C. Li, Z. Sun, W. Xu, R. Maingi, K. Tritz, D. Andruczyk, Y. Qian, Q. Yang, X. Yuan, J. Huang, X. Gao, B. Yu, J. Li, G. Zuo and J. Hu, "Real-time gas cooling of flowing liquid lithium limiter for the east", Fusion Eng. Des. **154**, 111537 (2020).

[22] J. Gerbeau, C. Bris and T. Lelièvre, *Mathematical Methods for the Magnetohydrodynamics of Liquid Metals, Numerical Mathematics and Scientific Computation* (Clarendon Press, 2006).

[23] J. Holman, *Heat Transfer* (McGraw-Hill., 5th ed., 1981).

[24] D. Griffiths, *Introduction to Electrodynamics, Pearson International Edition* (Prentice Hall, 1999).

[25] Y. Jaluria, *Computational Heat Transfer* (CRC Press, 2017).

[26] J. Hoffman, *Numerical Methods for Engineers and Scientists*, McGraw-Hill series in mechanical engineering (McGraw-Hill, 1992).

[27] P. Stangeby, *The Plasma Boundary of Magnetic Fusion Devices*, Series in Plasma Physics and Fluid Dynamics (Taylor & Francis, 2000).